GEOLOGICAL ANALYSIS OF THE VOLCANIC SUBSURFACE USING BOREHOLE RESISTIVITY IMAGES IN THE NGATAMARIKI GEOTHERMAL FIELD, NEW ZEALAND

Leon Halwa[1], Irene C. Wallis[2] and German Torres Lozada[1]

[1]Schlumberger, 256 St. Georges Tce, Perth, Australia 6000

[2]Mighty River Power, 283 Vaughan Road, Rotorua, New Zealand 3010

halwal1@slb.com

Keywords: *Borehole Imaging, Formation Micro-imaging, Resistivity Imaging, Fracture Analysis, Drilling Induced Fracturing, Drilling Enhanced Fracturing, Volcanic Fabric, Secondary Porosity*

ABSTRACT

Deploying wireline technology to evaluate the subsurface in New Zealand geothermal fields poses significant challenges owing to the dominantly volcanic setting and hostile well conditions. Despite this, a number of wireline logs were successfully collected during the 2011-2013 Ngatamariki Geothermal Field development drilling, including two high-quality resistivity-type borehole imaging logs. These kinds of borehole images are primarily used to characterize geological features such as *in-situ* stress direction, fractures (natural, drilling induced and enhanced) and the rock fabric. The fullbore formation micro-imager (FMI*) used at Ngatamariki is a pad-based tool that measures the electrical properties of rock and converts button resistivities to oriented electrical imagery of the borehole wall. This tool worked well at Ngatamariki because of the contrast between the low-resistivity drilling fluids and high-resistivity rock types present.

Image analysis included determining fracture type, orientation, density, aperture, fracture volumes, network relationship and, to a certain extent, fracture fill type. Resistivity characterisation allowed differentiation between potentially open and cemented fractures, as well as identification of both conductive and resistive cements. Because of the high resistivity contrast between the rock and drilling fluid, the physical properties of conductive and resistive clasts within the volcanic deposits could be described, and this facilitated dividing the images into textural zones. The presence and morphology of banding in pyroclastic and lava flow deposits was characterized by comparing sine wave morphology with textural heterogeneity. The FMI* logs collected at Ngatamariki provide an on-depth, high-resolution picture of the geological subsurface which is comparable to continuous core. As such they are a significant contribution to the understanding of the relationship between geological features and permeability, providing details that constrain both conceptual models and numerical simulations. The present study also represents advancement in resistivity image textural analysis techniques in volcanic deposits.

1. INTRODUCTION

1.1 Borehole Imaging in Volcanic Environments

Borehole imaging provides a high-resolution, oriented, false-colour map of the open borehole wall used for the petrophysical and geological evaluation of the subsurface. Borehole images are frequently used in the evaluation of the subsurface throughout the petroleum, mining, geothermal and hydrogeological industries (including other volcanic environments). There are several image technologies available, but those dominantly employed are based on either resistivity or acoustic principles. Wireline resistivity images are commonly used for detailed interpretations of natural fractures, *in-situ* stress directions, secondary porosity and rock fabric, as well as structural reconstructions of the subsurface.

Resistivity images rely on an adequate contrast in resistivity between geological features, as well as a high ratio of formation to mud resistivity. Variation in formation resistivity is due to changes in composition and proportion/morphology of void space, as well as the packing of particles in the rock mass. It follows that resistivity images can be employed for detailed identification of geologic features including bedding or flow banding, particle arrangement (from graded beds to brecciation textures), faults, fractures and even the nature of fracture fills. Ultrasonic images are based on the contrast of acoustic amplitude attenuation between the borehole wall and geological features. Acoustic images are frequently used to evaluate geological features that are more susceptible to acoustic attenuation, such as open fractures or less competent rock, as well as mapping the 360° shape of the borehole.

1.2 Borehole Imaging at Ngatamariki Geothermal Field

FMI* fullbore formation micro-images were obtained in two wells within the Ngatamariki Geothermal Field. These images were part of a comprehensive logging program undertaken during the 2011-2013 development drilling for 82-MW binary plant (Wallis *et al*. 2012). Ngatamariki is a 260°-285 °C, volcanic-rock hosted, geothermal resource located approximately 17 km north-east of Taupo. The geologic setting is an active volcano-tectonic rift (the Taupo Volcanic Zone) dominated by large-scale silicic volcanism overlying a fractured basement of meta-sandstone and argillite (Figure 1). The imaged well interval in the north intersects the following: (1) a sequence of tuffs (Tahorakuri Formation) and tuff breccias (Tahorakuri Formation with stipple) that is significantly altered with phyllic assemblage related to the intrusive complex and a later propylitic assemblage related to the current geothermal system (Lewis *et al*. 2012b); (2) an intrusive complex with multiple phases of intrusion; and (3) an as yet to be confirmed third formation (likely either andesite or basement greywacke) that is intensely fractured and altered by the adjacent intrusive. In contrast, the imaged interval in the south is not affected by the high-temperature, intrusive-related alteration assemblages and instead comprises the following: (1) a sequence of partially welded tuff (Tahorakuri Formation; Lewis *et al*. 2012c); (2) a short sequence of volcaniclastic

* Mark of Schlumberger

sediments not identifiable in the fine drill cutting returns; and (3) a pile of andesite lavas (Ngatamariki Andesite) and other associated deposits (block and ash deposits, breccias and a possible dike).

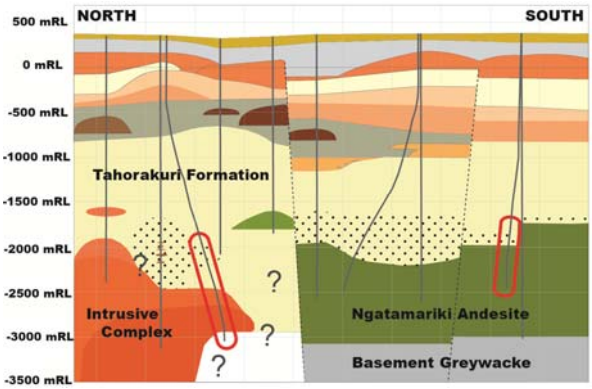

Figure 1. Simplified cross-section of Ngatamariki geology with relevant units labeled and the well intervals logged with the FMI* imager encircled in red. The stippled areas of the Tahorakuri Formation comprise andesite breccia, volcaniclastic breccias and sediments, or tuff breccias variably intercalated with pyroclastic deposits. Horizontal scale is approximately 5.5 km.

We found that the FMI* resistivity-based images are particularly well-suited to the identification of fractures at Ngatamariki. The bulk resistivity of volcanic rocks imaged at Ngatamariki is very high. Formation resistivity, as measured with an array induction tool (AIT*) run with the FMI* tool, was commonly up to 500 ohm.m, with some zones in the intrusive complex exceeding 2000 ohm.m. This high formation resistivity, combined with a drilling fluid resistivity of <5 ohm.m at logging temperatures, resulted in a favorable resistivity contrast for imaging.

The images acquired at Ngatamariki are not the first resistivity images collected in a hydrothermally altered volcanic environment (Davatzes *et al*. 2005; Stimac et al. 2010). Despite this, there is scarce technical literature that describes resistivity tool responses in this kind of environment. Our paper primarily focuses on bridging this gap in the literature by describing some of the key features of interest in these logs and challenges to interpretation. However, a short discussion covering some applications is provided for context.

2. FORMATION MICRO-IMAGER FUNDAMENTALS

The FMI* imager is a pad-based tool that uses 192 electrical buttons on its four pads and four flaps to produce a resistivity-based image. An applied voltage provides an alternating current from each of the 192 buttons, and this current will flow between the pads and an electrode on the upper cartridge housing. The current emitted from the pads is passively focused in the formation and follows a path that maximizes the volume of rock between the electrodes in order to capture the resistivity variations of the rock. The voltage potential is measured between electrodes and Ohm's law is used to determine the resistivity for each button.

The current that is recorded on the buttons is displayed as a series of curves that represent the resistivity variations of the formation. The buttons measure the electrolytic conduction and action exchange in the formation at a 0.1-inch (2.5-mm) sample rate, which in turn creates a conductivity variance curve of the formation. The button conductivity measurements are not calibrated quantitative measures of formation resistivity but are based on the conductive contrast of the formation. The variance curves are then converted to a false-colour image of the borehole that matches the resistivity to color scales (Hansen *et al* 2010; Bourke *et al* 1989). The image is a 360^{o} resistivity map of the borehole that is oriented by the use of a three axis accelerometer and magnetometer within the tool. Because the tool is pad based, the borehole coverage is inversely proportional to the size of the hole such that as the bit size increases, the pad coverage decreases. An 8.5-inch borehole has 78% pad coverage. Significant processing, such as adjusting for tool motion and orientation offsets, is required to prepare the image for geological interpretation. The processed image is a normalized (static and dynamic) color map wrapped around the borehole with the edges oriented at north and the center of the image at south (for north-oriented imagery). Relatively conductive features display darker color palettes, whereas resistive features are lighter in color. Images displayed in this paper are dynamic normalized images.

3. FRACTURE CHARACTERIZATION

Due to the aforementioned contrast between the rock and drilling fluid resistivity, the quality and detail of fracture imaging in the two logged intervals are very high. Several zones of micro-fractures are visible down to the millimeter scale, with the ability to distinguish fractures to 0.05mm (Schlumberger FMI* Technology Manuals 2002). The resistivity images in the Ngatamariki Geothermal field reveal an intensely fractured rock with complex fracture relationships.

3.1 Natural Fracture Analysis

With an overwhelming portfolio of fractures, dividing the fractures into sub-groups based on their physical character was the critical first step for meaningful interpretation. Consequently we classified fractures according to the trace length, type of infilling cement and their network relationship. The following describes some of the core differentiations made in our fracture classification scheme.

3.1.1 Types of fracture-infilling cement

Natural fractures occur as resistive (bright) or conductive (dark) traces on the FMI* images in water-based environments (Figure 2). Resistive fractures are likely filled with non-conductive minerals which commonly occur in geothermal environments such as quartz, calcite or anhydrite, but any highly resistive cement may occupy these fractures. Conductive fractures are often assumed to be open and potential pathways for permeability; however, these fractures may contain clay or other conductive minerals which commonly fill fractures in geothermal environments (Figure 2). Although it is not possible to discern if a conductive trace is an open or clay-filled fracture, we have identified a log artifact that allows us to identify which fractures may be filled with highly conductive cements such as pyrite or magnetite. Typically, conductive fractures appear as solid dark traces with well-defined borders (Figure 2B). However, some conductive fractures at Ngatamariki show a white rim surrounding their borders (Figure 2A). This white rim is referred to as a halo effect, and is caused by the build-up of excess current along the fracture due to materials with unusually high or low conductivity within the

fracture. Halo effects are more typically seen along fractures that are mineralized with resistive cements (Figure 2C) because the current does not flow easily across a resistive fracture (Lofts *et al*. 1999; Bourke *et al* 1989). The halo effect observed along some conductive fractures in the Ngatamariki images is not commonly seen in borehole images (Figure 2A). This buildup of excess current along a conductive fracture is interpreted to be a result of very high conductive cements in the fracture causing the current to pool along the fracture trace. We are interpreting this effect as an indicator of highly conductive minerals, such as pyrite or magnetite, within the fractures. We classified fractures with halos so they can be considered separately from purely conductive fractures due to their different implications when considering permeability.

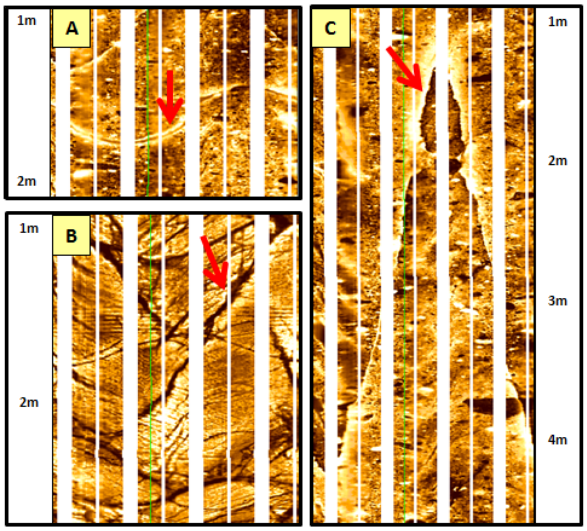

Figure 2: Image examples of natural fractures: (A) conductive fracture with halo effect and interpreted to be filled with pyrite of magnetite; (B) conductive fractures interpreted to be open or clay-filled; and (C) resistive fracture with halo effect, interpreted to contain resistive cements like quartz, anhydrite or calcite.

In the northern FMI* log, where the intrusive complex was intersected, we identified an unusual type of fracture morphology where a white resistive trace is surrounded with a conductive halo effect (Figure 3A). It occurs both in the intrusive and the surrounding tuffs and breccias with intense alteration. By using core recovered from the adjacent well as an analogue (Figure 3B), we have interpreted these features as resistive mineral-filled fractures surrounded by a clay alteration halo. This morphology of trace is not present in the southern well log and its occurrence is likely linked to the intrusive complex.

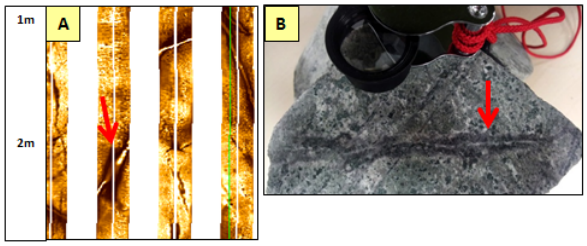

Figure 3: (A) FMI* image of a resistive fracture with a conductive halo along the fracture trace. This is interpreted to be a resistive-cement filled fracture with a clay alteration halo; (B) Core sample analogue where a quartz-albite vein hosted in volcaniclastic rock is surrounded by a chlorite rich alteration halo (mineral identification from Lewis *et al.* 2012a).

3.1.2 Trace length and network relationship

Some fractures fully cross cut the borehole while others extend partially across the borehole and show either truncation or cross cutting relationships with other fractures. Classifying fracture traces by extent and network relationship gives us a temporal framework that can be used in the investigation of the relative timing of fracture-forming events, such as large-scale intrusive or tectonic events, as well as insights into the history of the stress field. Furthermore, the complexity of the fracture network has an impact on permeability, tortuosity of the fluid pathway and the subsequent heat-mining capacity in the system.

3.1.3 Low-angle and bedding-parallel fractures

While the majority of the natural fractures imaged at Ngatamariki are high-angle or even sub-vertical (note that at Ngatamariki $S_v = \sigma_1$), we observed a smaller number of conductive fractures with lower dip magnitudes (<40°). These low-angle fractures often occurred in clusters (Figure 4A). We observed that the low angle fractures had two modes of occurrence. The first is where there is pronounced bedding or banding in the rock and the low angle fractures were oriented parallel to the bedding. In this instance the presence of low-angle fractures may be explained by failure occurring along a plane of weakness. If these bed-parallel conductive features are interpreted as open away from the borehole wall, then remaining open against the overburden stress could occur where the formation mechanical strength and asperities on the fracture surface are sufficiently great to prop-open the fracture against the overburden. Fluid pressures may also play a role, but geothermal systems are typically sub-hydrostatic. It is also possible that some low angle, bed-parallel fractures have been opened by unloading and thermal contraction at the borehole wall during drilling. This leads us to address the second mode of low-angle fracture occurrence; those which do not occur in well bedded intervals, nor are parallel to any visible pre-existing planes of weakness, but appear to cross cut all other features in the image, and at times show the appearance of crossing induced fractures (Figure 4C). The mechanism for these very low-angle (dip <20°) fractures are not clear, but may be a result of pressure release or exfoliation at the borehole wall due to unloading and thermal contraction during drilling. It is observed that these features are restricted to the intrusive formations and have similar characteristics to the disking seen in core extracted from the same formation in an adjacent well (Figure 4B).

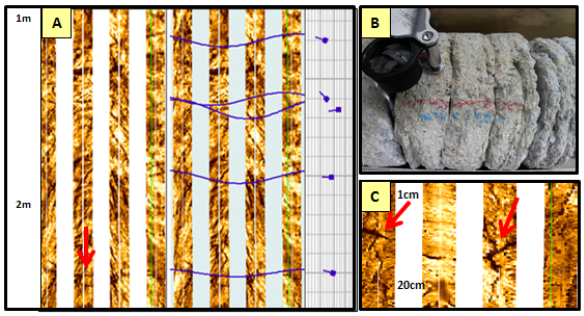

Figure 4: (A) Very low-angle conductive fractures in the images (tadpole scale 0-40 deg); (B) core from the same formation in an adjacent well which shows disking; and (C) low angle fracture appearing to cross an induced fracture.

3.3 Fracture Aperture Calculation

The volume of rock occupied by open fractures and the fracture distribution (a few large fractures or many small ones) are of key interest to the geothermal developer because they inform our understanding of the magnitude of thermal interaction between the fluid in fractures and the rock mass. Resistivity image interpretation gives us an understanding of both the distribution of fractures and a 2D volume calculated along the borehole wall, by calculating both the fracture aperture and fracture porosity. Fracture aperture calculations from resistivity images are calculated by quantifying the increased current flow in the fracture, which is mathematically modeled to determine aperture (Luthi *et al.* 1990). Modeling shows that the fracture aperture is proportional to the sum of the increased current flow (Grace *et al.* 1992). Combining the increased current with the mud and formation resistivity through a forward model provides a fracture width calculation (Luthi *et al.* 1990). Fracture porosity was then calculated along the borehole wall by multiplying the aperture by the fracture length (Grace *et al.* 1992).

Acoustic images can provide only qualitative estimations of fracture aperture because the acoustic attenuation cannot yet be quantified through empirical methods. Acoustic measurements are strictly confined to the surface of the borehole wall, compared to resistivity images, which considers a shallow depth of investigation in the resistivity calculations. The lack of empirical models for calculating aperture from acoustic attenuation restricts the ability to quantify the fracture width using this measure.

It was observed in the Ngatamariki study that the tuffs and sediments have larger aperture fractures than those located in the andesite, intrusive or intensely altered tuff deposits around the intrusive. However, these latter deposits contained much greater fracture frequencies than the tuffs and sediments.

3.5 Drilling-Induced Fracture Characterization

The Ngatamariki FMI* images contain significant drilling-induced fractures (DIF), but only rare, incipient wellbore breakout – a phenomenon not uncommon for high-temperature wells (e.g., Fernández-Ibáñez *et al*. 2009). The >200°C difference between the drilling fluid and reservoir rock temperatures creates significant tensile hoop stresses at the borehole wall and subsequently increases the likelihood of tensile failure at the wellbore wall while equally restricting compressive failure (cf. Zoback 2007). Care must be taken when interpreting images from this kind of stress environment, as there are examples of tensile fractures coalescing and hence appearing similar to borehole breakout.

DIF at Ngatamariki occur in three main types (Figure 5) and at various intensities. From these features we have determined the *in-situ* stress orientation (S_{Hmax} NE↔SW). Even in large borehole completions where borehole coverage is reduced, there is generally sufficient image coverage to capture the distribution of DIF (Figure 5B). We observed that shear en-echelon fractures are the most common type of DIF (Figure 5A, 5B), and that the overall distribution of DIF type correlates with the bulk-rock resistivity. Volcanics with more void space or larger amounts of clay alteration typically have decreased resistivity, and were found to be more dominated by echelon type failure. We observed that rock with a higher background resistivity, such as the andesite, diorite or welded zones in the Tahorakuri Formation, contains predominantly petal-centerline fractures (Figure 5D). It is likely that this high resistivity correlates with an increase in Young's modulus owing to lower void space and limited clay alteration. The frequency of petal-centerline fractures have been linked to the Young's modulus of rock as well as sudden increases in weight on bit (Kulander *et al*. 1990), where the latter is more likely to also occur in rock with increased strength. Simple tensile fractures were less common at Ngatamariki and occurred in limited zones throughout the field (Figure 5C).

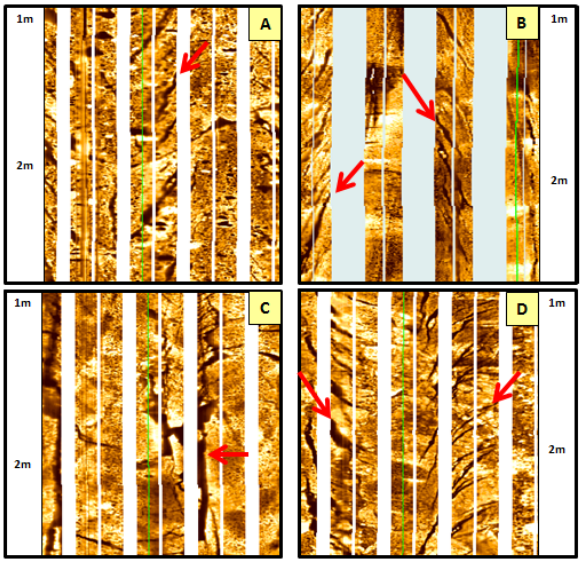

Figure 5: DIF seen in FMI* images in the Ngatamariki Geothermal field: (A) shear en-echelon failure in the Tahorakuri Formation (8.5" bit size); (B) shear en-echelon failure in Tonalite (12.25" bit size); (C) tensile failure in Ngatamariki Andesite; and (D) petal-centerline failure in Ngatamariki Andesite.

3.6 Drilling-Enhanced Fractures

In the Ngatamariki FMI* images we observe fractures that maintain the character and orientation of DIF, but the fracture traces are not restricted to the maximum stress directions (Figure 6). We have interpreted these as drilling enhanced fractures (DEF) – fractures that follow preexisting planes of weakness in the rock but have not been fully

developed or propagated until drilling. As a result, the fractures show a character that is more similar in appearance to induced fractures than natural fractures: they are commonly non-planar, display J-shaped splays and have irregular apertures or increased rugosity along the trace. DEF either partially or fully cross-cut the borehole depending on the extent of the preexisting plane of weakness. These features were excluded from geomechanical modeling at Ngatamariki because their orientation is influenced by the attitude of the preexisting weakness.

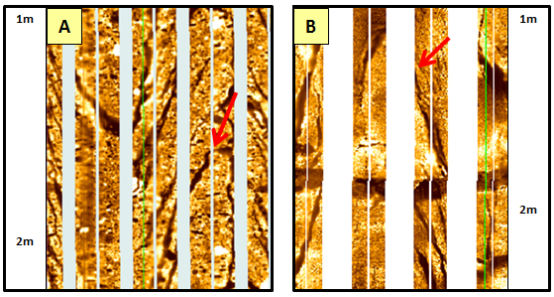

Figure 6: Drilling-enhanced fractures (DEF) in the FMI* images: (A) DEF in Tahorakuri 8.5" and (B) DEF in diorite 12.25"

4. ROCK FABRIC ANALYSIS

Resistivity images are the preferred wireline technology to characterise rock fabric in the subsurface, regardless of the geological environment. Resistivity images produce high-resolution azimuthal mapping of the borehole that closely compares to continuous coring. The bedding, laminations, flow banding, fiamme (welding textures), as well as various particle sorting, grading and breccias, are visible in FMI* images through variations in resistivity resulting from compositional, particle arrangement or void-space changes. Fabric is a key component of volcanic rock type identification because compositionally similar deposits can have different depositional processes and therefore fabric. Quantifying these physically different but chemically alike lithologies is of significant value to the geothermal operator because the physical arrangement of the rock is what dictates permeability character. Evaluation of image textures in Ngatamariki wells has revealed a wide range of rock fabrics from which zones could be defined. Characteristics such as clast size, sorting, proportion of conductive versus resistive clasts, fracture intensity, bedding density, clast shape and clast density were used as defining inputs for the construction of a series of rock fabric zones for each image. These zones are used to understand the formation history of the rocks and are a key component in ongoing work on understanding the relationships between rock types and permeability. The following section describes the key rock fabric groups identified in the Ngatamariki FMI* images and the impact of large-borehole completions on this analysis.

4.1 Bedding Analysis

The borehole images have been able to characterise the type, direction and thickness of lithological surfaces and layering in the rock. A bedding analysis in the Ngatamariki field has identified several kinds of bedding, including distinct well bedded surfaces, thinly spaced laminations, high-angle banding, flow banding, and several variations of subtle bedding and layering which was typically restricted to the Tahorakuri Formation.

4.1.1 Bedding in pyroclastic and volcaniclastic deposits

Bedding was identified in the pyroclastic and volcaniclastic deposits across a number of scales, from laminations to beds >0.5m thick. In the tuffs and ignimbrites it is difficult to differentiate between beds that are primary features and fabric that is related to digenetic or hydrothermal alteration processes (Figure 7A). Further work will be undertaken with the images to ascertain if the application of physical volcanology methods will reveal distinct eruptive units within the tuffs and perhaps even a flow direction for the ignimbrite deposits (Figure 7B). We observed high angle banding primarily within the volcaniclastics and this may represent post-deposition deformation events, such as fault-block rotation or slumping, or syndepositional processes such as the draping of deposits over paleotopography.

4.1.2 Flow banding in the andesite

Within the Ngatamariki Andesite, we identified unidirectional, laminated sections bounded by unconformable surfaces onto which the laminations truncate. These laminations have been interpreted as flow banding (Figure 8). If the rock has not been disturbed by post-depositional processes such as fault block rotation, their dip and azimuth represent the direction of lava flow within that lobe. The characterisation of flow directions within these extrusive deposits assists us with locating and paleotopography and possibly also vents.

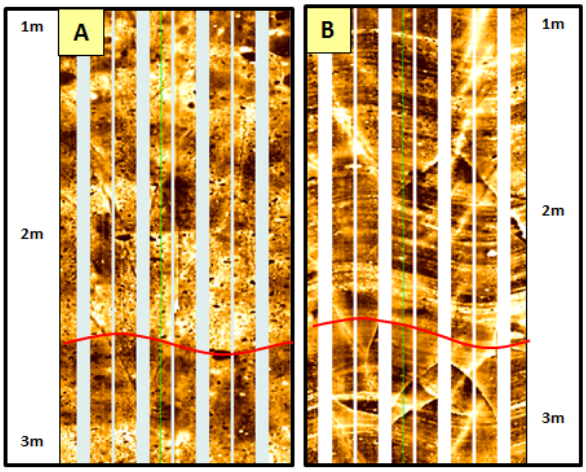

Figure 7: Bedding variability seen within the Tahorakuri Formation tuffs: (A) discrete and vague layered bands; and (B) thinly spaced laminated surfaces. The red lines highlight the bedding planes

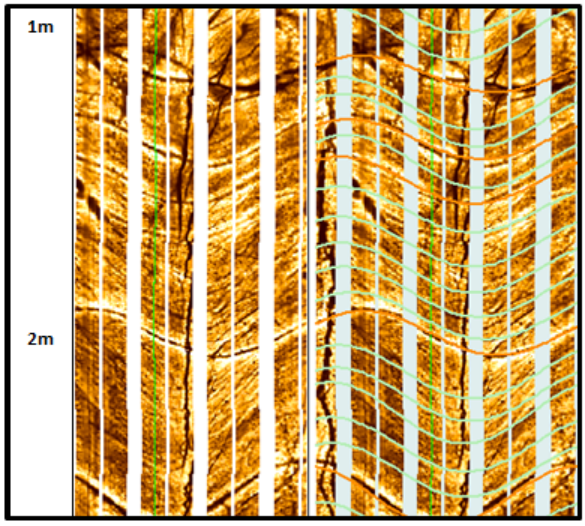

Figure 8: FMI* images showing an interpretation of flow banding (Green Sinusoids) within the andesite. This banding is bounded by unconformable surfaces (Orange Sinusoids) that represent the top and base of each flow unit.

4.1.3 Laminations

Laminations are very common throughout the images and are present in the FMI* images in several lithologies, including the pyroclastic, andesite, tonalite and diorite (Figures 7B, 8, 9, 10A). While the majority of the laminated surfaces were identified in the Tahorakuri Formation tuffs, they also were present in parts of the volcaniclastic and extrusive lava deposits. Laminated surfaces were dominantly uni-directional with distinct planar surfaces (Figure 7B, 10A). There were also laminations seen within the tuffs that displayed a more subtle fabric (Figure 9). These types of laminations maintained a planar character and showed faint resistivity contrast; however, they did not have the same apperance as flow banding (as seen in Figure 8). While the mechanism for the formation of these beds is not clear, they may be due to vatiations in alteration mineral depostion or diagenetic processes.

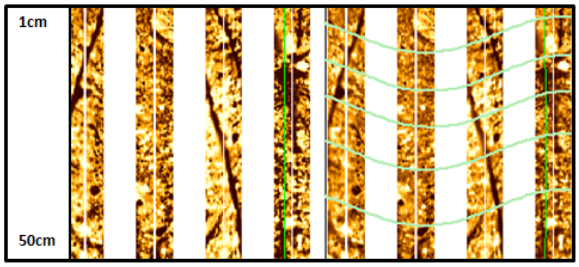

Figure 9: Subtle layering in tuff deposits (green sinusoids) could be a result of variable hydrothermal alteration or other diagenetic related processes.

4.2 Clast Arrangement

As expected, the fabric of the pyroclastic and volcaniclastic deposits is dominated by clasts, with a combination of conductive and resistive clasts of varying sizes, sorting and shapes. Some zones in the tuffs are dominated by larger conductive clasts which are likely to be clay-altered pumice similar to what is commonly observed in cores from this formation (Figure 10D). Other zones contain conductive clasts or irregularly shaped lenses accompanied by a halo effect (Figure 10B). The irregularly shaped lenses may be fiamme, representing a degree of welding in these intervals. The halo developing may indicate the presence of highly conductive minerals in these clasts and lenses. Several zones within the Ngatamariki Andesite are lithic rich, resistive, and clast-dominated (Figure 10E): a fabric that may be interpreted as syn- or post- deposition brecciation.

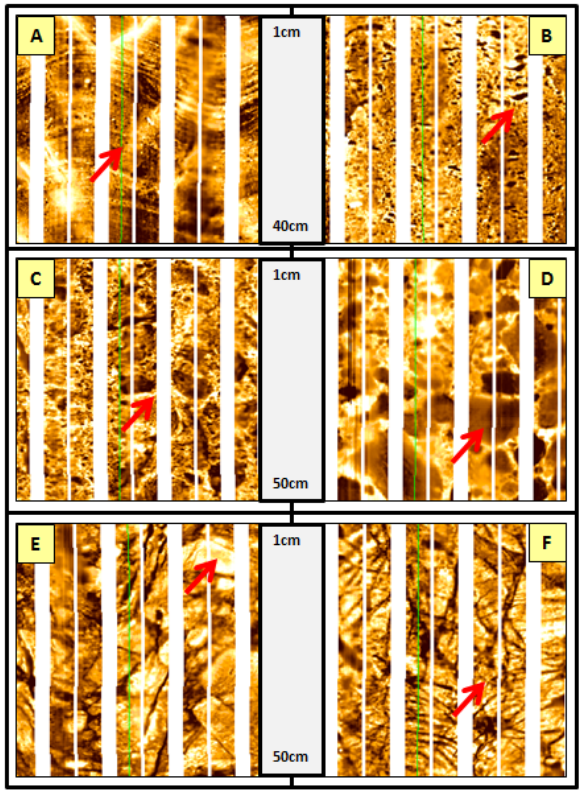

Figure 10: Selected rock fabric types seen in Ngatamariki resistivity images: (A) pyroclastic laminations; (B) conductive clasts with halo effect; (C) resistive rims surrounding conductive clasts; (D) angular conductive clasts; (E) resistive clast breccia; and (F) micro-fracturing .

The fabric variabililty in the images helped us to classify volcanic units which can be used to understand the depositional setting. The fabric variability also helped to identify discondant boundaries in both the volcanoclastic and extrusive intervals (Figure11).

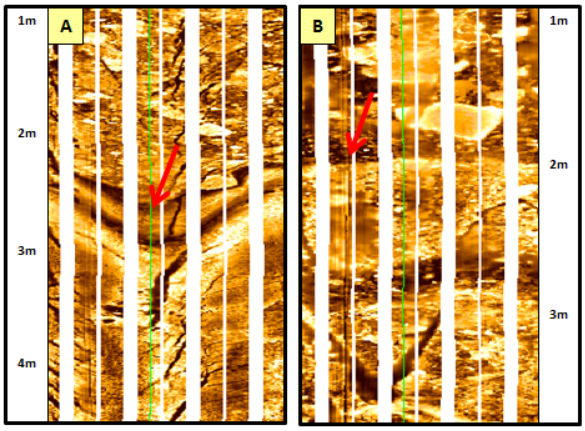

Figure 11: (A) Breccia (or block and ash deposit) overlying solid lava interpreted as either intrusive or a flow concomitant with deposition of the overlying deposit; (B) Volcaniclastic beds with various clast sizes and density that were later cross cut by a steeply dipping fracture.

4.3 Micro-fracturing

The FMI* logs contained zones of intense and complex micro-fracturing, which at times dominated the image. We define micro-fracturing as very small, commonly sub-millimeter erratic fracturing that does not conform to a fractured plane. They occur at many orientations and exists more as a mesh than a specific fracture plane. To capure this detail, we included microfracturing as a rock fabric category. The andesites are commonly micro-fractured (Figure 10F), as are the intrusive formations. In the pyroclastic deposits, we observed resistive micro-fracturing surrounding larger conductive clasts, suggesting that the matrix deformed in a brittle manner around the clast and was later mineralised (Figure 10C).

4.4 Fault Rocks

Borehole images are commonly used to identify structural deformation, and this is useful for understanding the tectonic history of the field. Traditional dipmeter logs formed the foundation for structural interpretations for several years, and imaging technologies have further complemented our ability to detect structural features. Acoustic images are not ideal for identifying bedding or fault associated fabrics (e.g., fault breccia), as in many cases these features lack acoustic attenuation contrast. Our success in identifying faults in the Ngatamariki Geothermal field increases with the use of resistivity imaging because textures associated with the fault zone become apparent. In the Ngatamariki images, it was common to see a variety of fault gouge and breccias ranging from micro-breccias through gouges and clast-rich fault breccis (Figure 12, Sibson 1977).

4.5 Textural Features from the Intrusive Complex

Image textures within the tonalite and diorite intrusive complex show some differences in the fabric. The diorite is extensively fractured but contains a large proportion of poorly sorted and angular clasts (Figure 13A). Some of the clasts show resistive borders that could indicate diagenetic mineralization, and several of the clasts show a conductive rim with a more resistive interior, which could be related to fractionation or post-deposition alteration. The tonalite was also intensely fractured, but commonly showed a speckled fabric with conductive specks dominating large sections of the lower intrusive (Figure 13B). The tonalite is also remarkably well-bedded, with the existence of laminations as well as thicker structural bedding. There was evidence of some localized ductile deformation in the tonalite with the appearance of a cylindrical fold (Figure 14). The structural bedding highlighted by the green sinusoids in Figure 14 shows a significant dip increased upwards, and a reversal of bedding dip direction above the fold. This 10-m local event highlights the deformed nature of the intrusive overall.

4.6 Textural Characterization in Larger Boreholes

FMI* images in Figures 3, 4, 5B, 6B, 9, 13, 14, and 15 were acquired in larger boreholes (12.25 inch). In larger boreholes, the pad coverage decreases and there is more space between the images. Despite the reduced image coverage, these figures demonstrate that the viability of rock fabric can still be captured. Figure 15A shows a resistive clast-rich zone of eye-shaped clasts (possibly fiamme) and Figure 15B highlights deformation textures common within the intrusive sequence.

5. DISCUSSION

The core aim of this paper is to describe some of the key features of interest in two FMI* image logs of hydrothermally altered volcanic terrain, and also some of the challenges in interpreting these images. However, a short discussion covering data applications for these images is provided below as context for why a geothermal operator would be interested in acquiring this kind of image.

It is commonly the case that geothermal drill cuttings returned to surface are small and mixed, if returned at all. Furthermore, overprinting alteration can make identification of the primary lithology challenging. Core acquisition is costly and provides a detailed snapshot of only that portion of the well. It follows that wireline logs have much to offer to complete the picture of sub-surface geology in geothermal fields (Wallis *et al*. 2012). Using FMI* logs we have been able to accurately locate lithologies not detectable though cutting analysis. For example, a sub-meter ash deposit, and potential marker horizon, was imaged within the Tahorakuri Formation. This feature is too small to be resolved though cuttings analysis. We have also located a sequence of volcaniclastic sediments overlying the Ngatamariki Andesite in a zone of poor-quality, fine cutting returns.

The conceptual and geologic models of a geothermal system provide guidance for well targeting and constraints for numerical simulations of heat and mass transfer in the reservoir. It follows that understanding the extent of each host rock and the permeability character of that rock is critical to successful resource development. Coupling a refined understanding of the stratigraphic sequence and distribution of fracture populations, with wireline measures of porosity (neutron, density and sonic logs) and fluid flow inside the wellbore, has enabled us to build numerically constrained conceptual models of permeability processes. The constraints are critical in making the conceptual models useful for numerical simulations; particularly by providing real-world constrains to parameters such as matrix porosity and fracture volume (i.e., the proportion of the model element defined as a fracture).

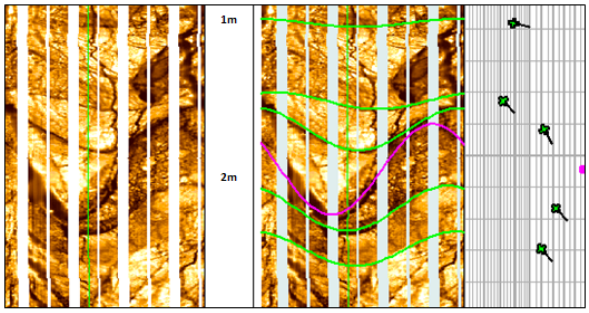

Figure 12: Fault breccia (>30% clasts) within the andesite with the fault surface defined (magenta sinusoid) and the dip of beds immediately above and below the fault noticeably steepened (green sinusoids and tadpoles).

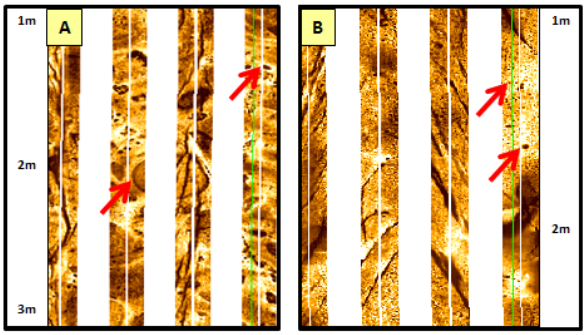

Figure 13: Intrusive rock fabrics: (A) clast rich diorite and (B) conductive clast speckled tonalite.

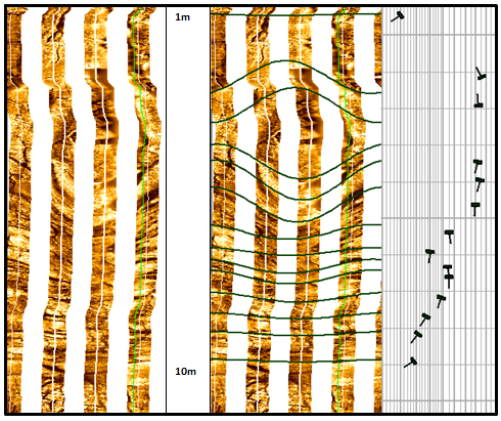

Figure 14: Structural deformation within the tonalite intrusive showing localized ductile folding. The green sinusoids represent the bedding surfaces which highlight the deformation.

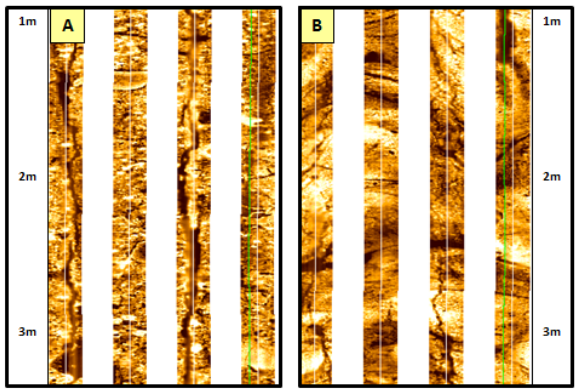

Figure 15: Resistivity images in 12.25-inch borehole completions showing textural variability in pyroclastic (left) and intrusive (right) rock fabric.

Thermal stimulation of geothermal wells (below the fracture pressure) is commonly observed, but not yet fully understood, phenomenon in geothermal wells. Models that describe the rate of thermal stimulation (e.g., Grant *et al*. 2013, Dempsey *et al*. in press) are valuable to a geothermal developer for well planning and management purposes. However, understanding when stimulation starts is part of predicting the rate of stimulation of a new injection well. The two resistivity image logs collected at Ngatamariki contain great numbers of both drilling induced and enhanced fractures. Although a sub-set of these are attributable to mechanical processes (e.g., petal-centerline fractures), the majority are related to thermal stresses from the difference between the formation and drilling fluid temperatures. These features are evidence that thermal stimulation of the wellbore is occurring during drilling.

6. CONCLUSION

The resistivity imaging at Ngatamariki was a successful venture that added significant detail to our understanding of the subsurface in that field. The images are high resolution owing to the resistivity contract between the volcanic formations and water-based drilling fluids. As well as characterising natural and drilling-induced fracturing, we were able to identify natural fractures that were enhanced during drilling. The drilling induced/enhanced features will provide key inputs to future geomechanical modeling and have improved our understanding of well stimulation during drilling.

Interpretation of these images characterised fracture types and orientation, differentiated between conductive and resistive cements, quantified fracture density and 2D volume (aperture and porosity) and defined fracture relationships within the volcanic formations. As such, these images are informing the conceptual model of this system and providing valuable inputs for the numerical models. The two image logs acquired at Ngatamariki also provided a detailed map of rock fabrics which were used to differentiate volcanic successions, even in large-borehole completions. As well as improving the resolution of the stratigraphic sequence, these successions can be employed during both genetic and 3D reconstructions of the geology.

ACKNOWLEDGEMENTS

The authors would like to acknowledge Mighty River Power for providing the data to conduct the study, and for the significant contribution they have made towards the study. The authors would also like to thank Schlumberger Ltd for providing the resources and time for the successful completion of the project.

REFERENCES

Bourke, L., Delfiner, P et al: *Using Formation MicroScanner Images* The Technical Review Publication Vol 37. No1 pp. 16-38 (1989)

Davatzes, N. C. and S. H. Hickman. *Comparison of acoustic and eletrical image logs from the Coso Geothermal Field, CA.* Thirtieth Workshop on Geothermal Reservior Engineering. Stanford University, Stanford, California. (2005)

Dempsey, D., Clearwater, J., Kellar, S. & Wallis, I. Validation of a coupled thermal-hydrological-mechanical model though a comparative study of sheer stimulation in two geothermal fields: Desert Peak, Nevada, USA and Ngatamariki, New Zealand. Elsewhere in this Volume.

Fernández-Ibáñez, F., Castillo, D., Wyborn, D., & Hindle, D., 2009. *Benefits of HT-Hostile Environments on Wellbore Stability: A Case Study from Geothermal Fields in Central Australia*. Proceedings Indonesian Petroleum Association, May 2009.

Grace, L.M et al.: *Geological Applications of Dipmeters and Borehole Images*. Schlumberger Technical Publications. (1992).

Grant, M.A., Clearwater, J., Quinão, J., Bixley, P.F., & Le Brun, M. *Thermal Stimulation of Geothermal Wells: A Review of Field Data.* Proceedings 38th Workshop on Geothermal Reservoir Engineering (2013)

Hansen, B. and Buczak, J. *Making Interpretable Images from Image Logs.* Chapter 4 in M. Poppelreiter, C. Garcia-Carballido, and M. Kraaijveld, *Dipmeter and borehole image log technology*: AAPG Memoir 92, p. 51-66. (2010)

Horne, R. N., *Modern Well Test Analysis – A Computer-Aided Approach.* Second Edition. Petroway, Palo Alto (1995)

Kulander, B.R., Dean, S.L. & Ward, B.J. Jr., *Fractured Core Analysis*. AAPG Methods in Exploration Series, No. 8. (1990)

Lewis, B., Chambefort, I. & Rae, A.J., *Geology of Injection Well NM8-NM8A, Ngatamariki Geothermal Field.* GNS Science Consultancy Report 2012/188 (2012a)

Lewis, B., Chambefort, I., Rae, A.J. & Sanders, F., *Geology of Injection Well NM9, Ngatamariki Geothermal Field.* GNS Science Consultancy Report 2012/330 (2012b)

Lewis, B., Chambefort, I., Rae, A.J. & Sanders, F., *Geology of Injection Well NM10, Ngatamariki Geothermal Field.* GNS Science Consultancy Report 2012/231 (2012c)

Lofts, J.C., and Bourke L.T., *The recognition of artefacts from acoustic and resistivity borehole imaging devices*. Geological Society of London, Special Publication Vol 159: 59-76 (1999)

Luthi, S.M., and Souhaite, P., *Fracture apertures from electrical borehole scans*. Geophysics Vol. 55. No.7 P. 821-833 (1990)

Schlumberger: *FMI – Borehole Geology, Geomechanics and 3D Reservoir Modeling*. Schlumberger Wireline Technology FMI Brochure SMP5822 (2002).

Sibson, R.H., *Fault rocks and fault mechanisms*. Journal of the Geological Society 133: 191-213 (1977).

Stimac, J. A., M. Baroek, Suminar, A.Sagala, B. Integration of surface and well data to determine structural controls on permeability at Salak (Awibengkok), Indonesia. Proceedings World Geothermal Congress Bali, Indonesia. (2010).

Wallis, I.C., McCormick, S., Sewell, S., & Boseley, C.: Formation Assessment in Geothermal Using Wireline Tools – Application and Early Results from the Ngatamariki Geothermal Field, New Zealand. Proceedings of the New Zealand Geothermal Workshop, Auckland. (2012).

Zoback, M.D., 2007, *Reservoir Geomechanics.* Cambridge University Press.